

Coulomb focusing in resonant production of super-ponderomotive photo-electrons from helium

H.G. Muller

*FOM-Institute for Atomic and Molecular Physics
Kruislaan 407, 1098 SJ Amsterdam, The Netherlands*

muller@amolf.nl

<http://www.amolf.nl/>

Abstract: We present wave functions of helium atoms exposed to an intense 800-nm laser, calculated by numerical integration of the time-dependent Schrödinger equation. Around 600 TW/cm² strong resonance enhancements of high-energy electrons occur, each leading to the appearance of specific quasi-periodic charge distribution patterns around the atom. The time-dependence of several such states is presented and discussed.

© 2001 Optical Society of America

OCIS codes: (020.0020) Atomic and molecular physics; (270.6620) Strong-field processes

References and links

1. B. Yang, K.J. Schafer, B. Walker, K.C. Kulander, P. Agostini and L.F. DiMauro, "Intensity - dependent scattering ring in above-threshold ionization," *Phys. Rev. Lett.* **71**, 3770 (1993).
2. P. Agostini, F. Fabre, G. Mainfray, G. Petite and N.K. Rahman, "Free-free transitions following six photon ionization of xenon," *Phys. Rev. Lett.* **42**, 1127 (1979).
3. K.C. Kulander, K.J. Schafer and J.L. Krause, "Time-dependent studies of multiphoton processes," in *Atoms in intense laser fields*, ed. M. Gavrila, Academic (1992) p.247; K.J. Schafer and K.C. Kulander, "Energy analysis of time-dependent wave function: Application to above threshold ionization," *Phys. Rev. A* **42** (1990) 5794.
4. H.G. Muller, "Tunneling excitation to resonant states in helium as the main source of super-ponderomotive electrons in the tunneling regime," *Phys. Rev. Lett.* **83**, 3158-61 (1999).
5. H.G. Muller and M.V. Fedorov, *Super-Intense Laser-Atom Physics V* proceedings, NATO series, p. ix Wolters-Kluwer Academic Publishing, (1996).
6. H.G. Muller, "An efficient propagation scheme for the time-dependent Schrödinger equation in the velocity gauge," *Laser Phys.* **9**, 138 (1999).
7. H.B. van Linden van den Heuvell and H.G. Muller, "Limiting cases of excess-photon ionization," in S.J. Smith and P.L. Knight (eds.), "Studies in Modern Optics No. 8, *Multiphoton processes*", p. 25-34, Cambridge University Press, Cambridge, (1988).
8. G.G. Paulus, W. Nicklich, Huale Xu, P. Lambropoulos and H. Walther, "Plateau in above threshold ionization spectra," *Phys. Rev. Lett.* **72** (1994) 2851.
9. P.B. Corkum, "Plasma perspective on strong field multiphoton ionization," *Phys. Rev. Lett.* **71** (1993) 1994.
10. H.G. Muller, "Numerical simulation of high-order above-threshold-ionization enhancement in argon," *Phys. Rev. A* **60**, 1341-50 (1999).
11. M. Pont, N. Walet, M. Gavrila and C.W. McCurdy, "Dichotomy of the hydrogen atom in super-intense, high-frequency laser fields," *Phys. Rev. Lett.* **61**, 939 (1988)
12. T. Brabec, M.Yu. Ivanov and P.B. Corkum, "Coulomb focusing in intense field atomic processes," *Phys. Rev. A* **54**, R2551-R2554 (1996).

1 Introduction.

Recently, it was discovered that photoionization of helium with 800-nm light can produce electrons with an energy of several hundred eV[1]. This energy is obtained through absorption of hundreds of photons, a phenomenon known as above-threshold ionization

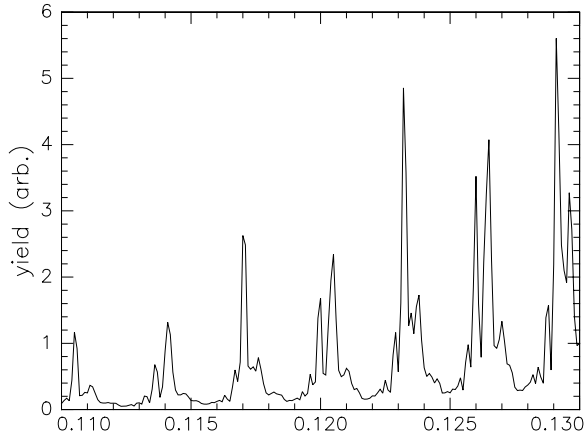


Fig. 1. Yield of electrons with energies larger than 100 eV as a function of the electric field amplitude E_0 .

(ATI) [2]. A fully quantum-mechanical calculation of the ionization process in the framework of the single-active-electron approximation (SAE)[3] predicts that the production of such electrons is mediated by narrow resonances[4], which enhance the process at very specific intensities (Fig. 1).

The states responsible for the enhancement are very weakly bound to the atom, with a binding energy of about 800 meV. This stands in sharp contrast to the enormous kinetic energies that free and weakly bound electrons get due to the oscillating 'quiver' motion they engage in under the influence of the laser. In the intensity range of interest (400-600 TW/cm²), the cycle-average energy due to this motion, (the ponderomotive energy U_p), is the equivalent of about 20 photons (30 eV). The resonant states thus do exist in a regime where the laser is the dominant factor determining electron motion, and completely overwhelms the intra-atomic forces. This super-intense regime [5] leads to interesting behavior that is highly dynamic and strongly differs from ordinary atomic structure.

In this paper we present the dynamics of the time-dependent wave functions Ψ of the resonant states responsible for the observed enhancement of the production of the high-energy electrons, as revealed by numerical solution of the time-dependent Schrödinger equation

$$i \partial_t \Psi(t) = H(t) \Psi(t) \quad (1)$$

on a grid[3]. The hamiltonian $H(t)$ in this equation models the helium atom as a single electron in a potential well V (representing the nuclear attraction and its screening by the other electron frozen in an ionic $1s$ state[4]), in the presence of a time-dependent homogeneous electric field described by the time-dependent vector potential $A(t)$, i.e.

$$H(t) = \frac{1}{2} p^2 + V + A(t) \cdot p. \quad (2)$$

The ensuing partial differential equation is solved numerically on a radial-position, angular-momentum grid with absorbing boundary conditions at the radial outer edge, by a unitary multiply split-operator method described elsewhere[6]. To obtain convergence, 120 angular momenta and 1000 radial grid points (spaced by $\delta r = 0.15$ Bohr) were used, at a time step of about 0.055 a.u. (2000 steps per optical cycle).

2 Results and discussion.

The dominant electron flux emitted by the ionizing helium atom consists of 'primary' electrons with a kinetic energy below 2-3 times U_p . Such electrons can be formed by straightforward ionization (through a field-induced tunneling process), followed by acceleration of the quasi-free electron in the laser field[7]. Typically, the production of high-energy electrons, with energies in the range 3-10 U_p , is 2 to 3 orders of magnitude smaller. This region of the electron spectrum is known as the ATI-plateau[8], and originates from primary photo-electrons that boost their energy in a rescattering event with their parent ion[9]. It is the production of these electrons that can be resonantly enhanced at several precisely determined intensities[4].

In order to bring out the resonant charge density amidst the much larger flux of outgoing low-energy electrons, a projection technique is used. An atom in its ground state is exposed to a laser pulse that, after a short (half-cycle) turn-on, has a constant-amplitude electric field $E(t) = E_0 \cos \omega t$. After 20 cycles of constant intensity, transient effects due to the turn-on have expired, and a quasi-stationary state develops on the entire grid all the way up to its absorbing boundary. At a zero-crossing of the electric field, the wave function is orthogonalized on a (suitably polarized) ground-state wave function[10]. This removes more than 99% of the electronic charge. What is left consists of the excited and ionized products created during the most recent part of the 20-cycle period.

The wave function is then propagated a few (3-5) more cycles. This is sufficient to have the low-energy primary-electron flux move out of the immediate vicinity of the atom, and have it absorbed by the boundary. The production of new flux of this type of course ended with the removal of the ground state. What is left then is the bound-state charge density that has built up during the 20-cycle period, and the ionization products that stem from this charge density (the electrons responsible for the plateau enhancement).

Due to this ionization, which seems to have an approximately flat energy spectrum stretching from 0-8 U_p , the resonant states decay quite rapidly: their norm shrinks by between 20 and 30% per optical cycle. The presented movies are corrected for this decay by changing the density-scale of the contour plot exponentially with time, in such a way that the behavior becomes periodic. A single cycle can then be repeated indefinitely, and such a single-cycle movie gives a good impression of the nature of the resonant state and its mode of decay.

Indeed, the wave functions that result from this procedure are a very wild function of intensity, both in norm and in character. Each enhancement peak in Fig. 1 corresponds to a completely different charge distribution. Away from enhancements, the norm of this charge distribution is correspondingly smaller. All the wave functions have in common that they extend over a region of about 100 Bohr across, and since the Coulomb well is not very deep at such distances, they can only be very weakly bound. In particular, the Coulomb forces are no match for the laser, and can not prevent the charge in the states to be driven into a similar quiver motion as a free electron would be; at the relevant intensities the amplitude α_0 of this motion is about 40 Bohr units.

In the present case of linear polarization, the charge densities are cylindrically symmetric. All plots thus only have to give the charge density in a plane through the polarization axis. There are several ways to do this. The true charge density $|\Psi|^2$ can be plotted, but this would make charge moving away from the axis quickly decrease in density, because it spreads out as rings around the symmetry axis. Alternatively, one can take the volume element $\rho d\rho$ of cylindrical coordinates (z, ρ, ϑ) into account, by plotting $\rho |\Psi|^2$. This faithfully represents the total amount of charge, and thus prevents

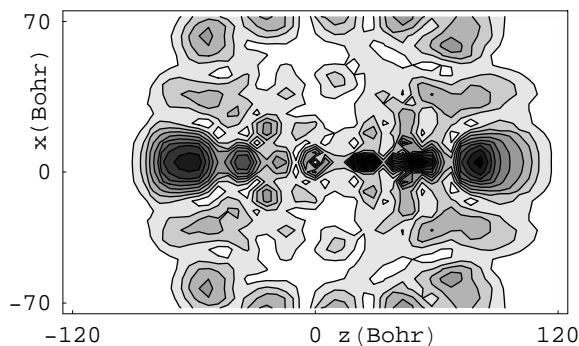


Fig. 2. Resonance charge distribution at $E_0 = 0.1284$ a.u., which is obtained from the total wave function after removal of the ground state and primary continuum electrons. The state quivers over a distance of 40 Bohr in either direction, and avoids contact with the nucleus almost entirely. (Movie size 1.2 MB)

this apparent disappearance of off-axis charge density. This way of plotting forces an artificial 'nodal line' at $\rho = 0$, however, making it impossible to observe the behavior on the axis. The plots presented here use a compromise, by plotting $|\Psi|^2 \sqrt{36 + \rho^2}$, which fixes the shortcomings of the other methods at the expense of introducing an arbitrary constant (which in practice was picked just large enough to suppress any splitting of the on-axis charge lobes).

In Fig.2 a high angular-momentum state is shown, that occurs at $E_0 = 0.1284$ a.u.. It avoids the nucleus quite well, and as a result only gives rise to very few high-energy ionization products (which can only originate by large momentum transfer between electron and nucleus, which requires a close approach). Although there is some enhancement visible in the high-energy electron production at this intensity, it is comparatively small. The total charge in the resonant cloud, however, is similar to that of other resonances.

Fig. 3 and 4 show the resonant charge distribution at $E_0 = 0.01296$, (a 2% higher intensity!). This state has a completely different nature. Most of the charge density is on the polarization axis, leading to a strong interaction with the nucleus. It can be seen quite well in the accompanying 3-D movie how the the various lobes of the wave funct-

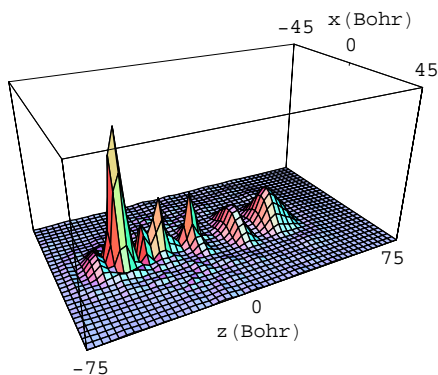


Fig. 3. The resonance charge distribution at $E_0 = 0.01296$ a.u., which consists of five on-axis blobs that quiver over a distance of 40 Bohr in either direction. The movie (1.1 MB) shows how the charge density is revived as the lobes are focused on passing the nucleus.

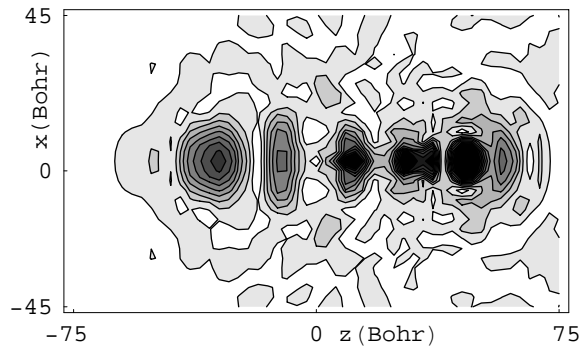


Fig. 4. The same resonance charge distribution as in Fig. 3 (at $E_0 = 0.1296$ a.u.), but shown as a contour plot, in which the decay products can be observed more clearly. (Movie size 1 MB.)

ion spread as they move far away from the nucleus, but are 'revived' as they pass it close by, and some population (passing too close) is scattered out of it at large angles. This breathing of the charge lobes is the main effect of the finite frequency; in the high-frequency limit [11] the shape of the wave function would be completely stationary and without any decay.

The resonances of Fig. 2 and Fig. 3/4 are extremes; intermediate forms, having both on-axis and off-axis components occur as well. Fig. 5, obtained at $E_0 = 0.1291$ a.u. shows an example. A quite strange structure is visible in Fig. 6, at $E_0 = 0.1265$ a.u.: here the charge consists of two spherical shells, each surrounding a strong charge blob. In contrast to the states shown in Fig. 2-5, which were all excited by absorption of 38 photons, the state in Fig. 6 is in 37-photon resonance with the ground state. As a consequence, it has opposite parity, showing up as an extra nodal plane perpendicular to the axis.

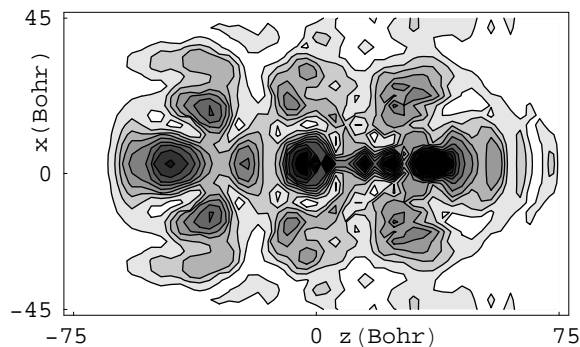


Fig. 5. The resonance at $E_0 = 0.1291$ a.u., which shows both on-axis and off-axis features, plotted in the same way as Fig. 4. (Movie size 1.2 MB)

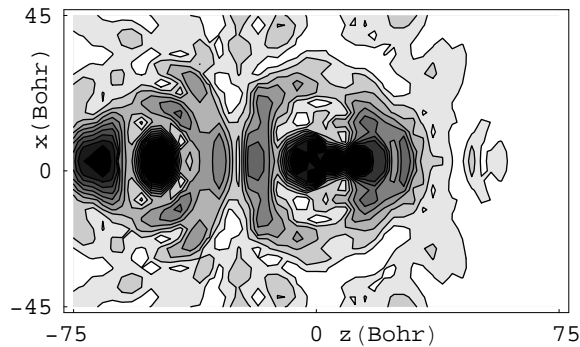


Fig. 6. The resonant charge density at $E_0 = 0.1265$ a.u., plotted as in Fig. 4. (Movie size 1.3 MB) Note the small packet of fast electrons leaving along the axis.

In the movie behind Fig. 6 it can be seen how scattering occurs on collision with the nucleus. Since most charge is displaced quite far from the nuclear position at zero field, it encounters the nucleus at two unequally spaced times during the optical cycle. The first encounter sees a relatively smooth charge distribution colliding with the nucleus. This encounter focuses the charge onto the axis, leaving a wake of high charge density in the nuclear trail. This charge density is 'set up' for a hard collision with the nucleus when the quiver velocity reverts a short time later, resulting in a lot of backscattering. A very fast outgoing blob of probability can be seen leaving the picture along the axis.

3 Conclusions.

Although earlier studies assumed that only the first encounter of an escaping wave packet is important for backscattering, it seems that focusing of the charge cloud by the attractive tail of the Coulomb potential is a major factor enhancing later collisions[12]. This focusing can occur in a weak, long-range form that is responsible for 'shepharding' the charge-cloud of zero drift momentum in such away that it continues to hang around the nucleus for many cycles. A second manifestation of this focusing is able to set up for a short time a large charge density on the axis by forward scattering, that can impact the nucleus face on. This results in a large enhancement of the backscattering out of the state.

The whole process of formation of the resonant charge cloud and its subsequent decay by scattering is dominated by hydrogenic dynamics, since it happens at a distance so large that the short-range part of the potential responsible for the quantum defect of low- ℓ Rydberg states has no effect. Hydrogen thus could support similar excited states in the laser field. The tightly bound ground state of helium, however, is essential for feeding population into these states at the high intensity were they occur: in hydrogen the ground state would ionize to completion long before the intensity reaches 200 TW/cm^2 .

Acknowledgement - I am indebted to Matt Kalinski for helping me to produce the movies. This work is part of the research program of the foundation fo Fundamental Research on Matter (FOM), which is subsidized by the Netherlands organization for the Advancement of Research (NWO).